NASA/CR-2002-211762
ICASE Report No. 2002-28

P_1 Nonconforming Finite Element Method for the Solution of Radiation Transport Problems

Kab Seok Kang
ICASE, Hampton, Virginia

August 2002

The NASA STI Program Office . . . in Profile

Since its founding, NASA has been dedicated to the advancement of aeronautics and space science. The NASA Scientific and Technical Information (STI) Program Office plays a key part in helping NASA maintain this important role.

The NASA STI Program Office is operated by Langley Research Center, the lead center for NASA's scientific and technical information. The NASA STI Program Office provides access to the NASA STI Database, the largest collection of aeronautical and space science STI in the world. The Program Office is also NASA's institutional mechanism for disseminating the results of its research and development activities. These results are published by NASA in the NASA STI Report Series, which includes the following report types:

- TECHNICAL PUBLICATION. Reports of completed research or a major significant phase of research that present the results of NASA programs and include extensive data or theoretical analysis. Includes compilations of significant scientific and technical data and information deemed to be of continuing reference value. NASA's counterpart of peer-reviewed formal professional papers, but having less stringent limitations on manuscript length and extent of graphic presentations.

- TECHNICAL MEMORANDUM. Scientific and technical findings that are preliminary or of specialized interest, e.g., quick release reports, working papers, and bibliographies that contain minimal annotation. Does not contain extensive analysis.

- CONTRACTOR REPORT. Scientific and technical findings by NASA-sponsored contractors and grantees.

- CONFERENCE PUBLICATIONS. Collected papers from scientific and technical conferences, symposia, seminars, or other meetings sponsored or cosponsored by NASA.

- SPECIAL PUBLICATION. Scientific, technical, or historical information from NASA programs, projects, and missions, often concerned with subjects having substantial public interest.

- TECHNICAL TRANSLATION. English-language translations of foreign scientific and technical material pertinent to NASA's mission.

Specialized services that complement the STI Program Office's diverse offerings include creating custom thesauri, building customized data bases, organizing and publishing research results . . . even providing videos.

For more information about the NASA STI Program Office, see the following:

- Access the NASA STI Program Home Page at ***http://www.sti.nasa.gov***

- Email your question via the Internet to help@sti.nasa.gov

- Fax your question to the NASA STI Help Desk at (301) 621-0134

- Telephone the NASA STI Help Desk at (301) 621-0390

- Write to:
  NASA STI Help Desk
  NASA Center for AeroSpace Information
  7121 Standard Drive
  Hanover, MD 21076-1320

NASA/CR-2002-211762
ICASE Report No. 2002-28

P_1 Nonconforming Finite Element Method for the Solution of Radiation Transport Problems

Kab Seok Kang
ICASE, Hampton, Virginia

ICASE
NASA Langley Research Center
Hampton, Virginia

Operated by Universities Space Research Association

Prepared for Langley Research Center
under Contract NAS1-97046

August 2002

Available from the following:

NASA Center for AeroSpace Information (CASI)
7121 Standard Drive
Hanover, MD 21076-1320
(301) 621-0390

National Technical Information Service (NTIS)
5285 Port Royal Road
Springfield, VA 22161-2171
(703) 487-4650

P_1 NONCONFORMING FINITE ELEMENT METHOD FOR THE SOLUTION OF RADIATION TRANSPORT PROBLEMS

KAB SEOK KANG*

Abstract. The simulation of radiation transport in the optically thick flux-limited diffusion regime has been identified as one of the most time-consuming tasks within large simulation codes. Due to multimaterial complex geometry, the radiation transport system must often be solved on unstructured grids. In this paper, we investigate the behavior and the benefits of the unstructured P_1 nonconforming finite element method, which has proven to be flexible and effective on related transport problems, in solving unsteady implicit nonlinear radiation diffusion problems using Newton and Picard linearization methods.

Key words. nonconforming finite elements, radiation transport, inexact Newton linearization, multigrid preconditioning

Subject classification. Applied and Numerical Mathematics

1. Introduction. Radiation transport in astrophysical phenomena and inertial confinement fusion is often modeled using a diffusion approximation [12, 17, 18, 20, 21, 22, 24]. When the radiation field is not in thermodynamic equilibrium with the material a coupled set of time dependent diffusion equations is used to describe energy transport. These equations are highly nonlinear and exhibit multiple time and space scales. Implicit integration methods are desired to overcome time step restrictions.

Nonconforming finite-element methods have proven flexible and effective on incompressible fluid flow problems such as incompressible Stokes and Navier-Stokes equations [10, 11]. In the P_1 nonconforming method, the degrees of freedom lie on midpoints of edges. Therefore, the number of connections of degrees of freedom with each others at most four (four at interior edges and two at boundary edges) which is the same number of connections of degrees of freedom in structured finite difference methods. In contrast, in the P_1 conforming method, the number of connections of degrees of freedom is at least four except at boundary points, and depends the triangulation and position of points. The number of connections of degrees of freedom determines the number of nonzero entries of generated matrices and plays an essential role in performance of parallel implementations because of the communication required in kernel operations like matric-vector multiplication. P_1 nonconforming methods generate matrices that have a constant small number of nonzero entries for each row, and therefore have some advantages in parallel implementation and performance.

Because many nonlinear elliptic problems are well solved by conforming finite element methods, nonconforming methods are still rare for such problems. However nonconforming methods may resolve features of solutions of nonlinear problems not well represented by conforming methods. In this research, a nonconforming methodis shown to resolve very sharp changes of energies on heterogeneous domains. The results are very similar to the solutions of the finite volume method with an edge-based flux limiter [19].

To solve nonlinear problems, one usually employs linearization techniques. Many modelers use Picard and Newton methods to linearize. Picard's method is easy to understand and implement, but converges

*ICASE, Mail Stop 132C, NASA Langley Research Center, Hampton, VA 23681-2199 **email: kks002@icase.edu**. This research was partially supported by the National Aeronautics and Space Administration under NASA Contract No. NAS1-97046 while the author was in residence at ICASE, NASA Langley Research Center, Hampton, VA 23681-2199. This work was also partially supported by postdoctoral fellowships program from Korea Science & Engineering Foundation (KOSEF).

slowly. Newton's method has a second-order convergence rate but requires the Jacobian of the original nonlinear system. In many nonlinear problems, an inexact Newton method works well, with less storage and operation count expense [8]. In this paper, we study the behavior of these three methods on a model radiation transport problem.

Because the system generated from some linearization of the nonlinear problem is usually nonsymmetric, we use preconditioned GMRES [23]. As a preconditioner, we consider multigrid. Multigrid represents an important advance in algorithmic efficiency for the solution of large problems [2, 3, 4, 14, 19, 25].

To use multigrid, we need to define intergrid transfer operators between nonconforming finite-element spaces. Due to the non-nestedness of nonconforming spaces, there is no natural intergrid transfer operator. In previous studies of the nonconforming multigrid method, the average value of two adjacent elements is used to get the interpolated value at a node. Nonconforming multigrid with this intergrid transfer operator is a good solver for linear systems and some nonlinear systems with smooth nonlinear coefficients [1, 5, 6, 9, 15, 16]. However this intergrid transfer operator does not preserve positivity of functions, which is an essential part of radiation transport problems because energy and temperature are always positive. Therefore some nonlinear problems with discontinuous coefficients, bound constraints on solutions, and rapidly changing solutions, like the radiation transport problem, cannot use this intergrid transfer operator because the coarse level approximation obtained from the fine level approximation does not satisfy solution bounds, and one cannot generate the coarse level systems or solve the coarse level problems [15]. To overcome these difficulties, we use a new and simple intergrid transfer operator that preserves positivity and solves the above mentioned problem. However multigrid with this intergrid transfer operator is slower than with the previous operator. Therefore, we use the simple intergrid transfer operator to derive coarse level systems and the average value intergrid operator to solve the linear systems.

The rest of the paper is organized as follows. In section 2, we describe a model radiation transport and its P_1 nonconforming discretization. In section 3, we consider a discretization in time, derive the linearizations by Picard and Newton method, and describe the Inexact Newton method. In section 4, we describe preconditioned GMRES and the nonconforming multigrid preconditioner. Numerical experiments are given in section 5.

2. Radiation transport model and P_1 nonconforming discretization. Under the assumption of an optically thick medium (short mean free path of photons) a first-principles statement of radiation transport reduces to the radiation diffusion limit. A particular idealized dimensionless form of such a system, known as the "2T" model, can be written as:

$$\frac{\partial E}{\partial t} - \nabla \cdot (D_r \nabla E) = \sigma_a (T^4 - E), \tag{2.2.1}$$

$$\frac{\partial T}{\partial t} - \nabla \cdot (D_t \nabla T) = -\sigma_a (T^4 - E), \tag{2.2.2}$$

with

$$\sigma_a = \frac{z^3}{T^3}, \quad D_r(T,E) = \frac{1}{3\sigma_a + \frac{1}{E}|\nabla E|}, \quad \text{and } D_t(T) = \kappa T^{\frac{5}{2}}. \tag{2.2.3}$$

Here, $E(x,t)$ represents the photon energy, $T(x,t)$ is the material temperature, σ_a is the opacity, and κ is the material conductivity. In the non-equilibrium case, the nonlinear source terms on the right-hand side are nonzero and govern the transfer of energy between the radiation field and material temperature. Additional nonlinearities are generated by the particular form of the diffusion coefficients, which are functions of the E and T fields. In particular, the energy diffusion coefficient, $D_r(T,E)$ contains the term $|\nabla E|$ which

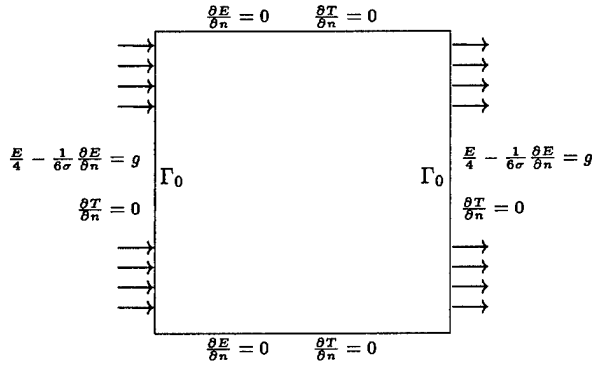

FIG. 1. *Domain of model problem*

refers to the gradient of E. This limiter term is an artificial means of ensuring physically meaningful energy propagation speeds (i.e. no faster than the speed of light). The atomic number z is a material coefficient, and while it may be highly variable, it is only a function of position (i.e. $z = f(x, y)$ in two dimensions).

The two model problems considered in this study are taken from [19] and depicted in Figure 1. We consider a unit square domain of similar material with atomic number $z = 1$ and a unit square domain of two dissimilar materials, where the outer region contains material with an atomic number of $z = 1$ and the inner region ($1/3 < x < 2/3$, $1/3 < y < 2/3$) contains material with an atomic number of $z = 10$. The top and bottom walls are insulated, and inlet and outlet boundaries are specified using mixed (Robin) boundary conditions, as shown in the figure. For convenience, we represent the boundary $x = 0$, $0 \le y \le 1$ and $x = 1$, $0 \le y \le 1$ by Γ_0, and otherwise by Γ_1. Then the boundary condition of the problem is

$$\begin{aligned} \frac{E}{4} - \frac{1}{6\sigma_a}\frac{\partial E}{\partial n} &= g, \quad \text{on } \Gamma_0, \\ \frac{\partial E}{\partial n} &= 0, \quad \text{on } \partial\Omega - \Gamma_0, \\ \frac{\partial T}{\partial n} &= 0, \quad \text{on } \partial\Omega, \end{aligned}$$

where n is the local outward normal vector of the boundary.

Equations (2.2.1) and (2.2.2) form a system of coupled nonlinear partial differential equations which must be discretized in space and time. In this section, we consider a discretization in space and will consider a discretization in time in the next section.

The variational form of (2.2.1) and (2.2.2) can be written as follows: Find $(E, T) \in (H^1(\Omega) \cap L^2([0, T]))^2$ such that

$$\begin{aligned} \int_\Omega \frac{\partial E}{\partial t} u dx + \int_\Omega D_r \nabla E \cdot \nabla u dx + \int_{\Gamma_0} \frac{1}{2} E u d\sigma \\ - \int_\Omega \sigma_a((T)^4 - E) u dx - \int_{\Gamma_0} 2 g u d\sigma = 0, \end{aligned} \tag{2.2.4}$$

$$\int_\Omega \frac{\partial T}{\partial t} v dx + \int_\Omega D_t \nabla T \cdot \nabla v dx + \int_\Omega \sigma_a((T)^4 - E) v dx = 0, \tag{2.2.5}$$

for all $(u, v) \in (H^1(\Omega))^2$ and for all $t \in [0, t\text{max}]$.

We discretize Ω by using a triangular grid containing edges, shown in Figure 2. The grid is generated by connecting of the midpoints of the edges of the triangles from the coarsest discretization $\mathcal{T}_1$, which contains

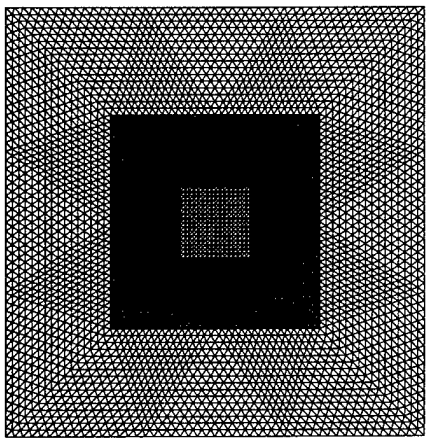

FIG. 2. *Discretization of Domain*

edges and conforms to the material interface boundaries in such a way that no triangle edges cross this boundary. Let h_j and $\mathcal{T}_{h_j} \equiv \mathcal{T}_j$, for $j = 1, \ldots, J$, be given, where $\mathcal{T}_j$ is a partition of Ω into triangles and h_j is the maximum diameter of the elements of $\mathcal{T}_j$.

Define the P_1-nonconforming finite element spaces

$$V_j = \{v \in L^2(\Omega) : v|_K \text{ is linear for all } K \in \mathcal{T}_j, \\ v \text{ is continuous at the midpoints of interior edges}\}.$$

Then the nonconforming finite element discretization of (2.2.4) and (2.2.5) can be written as : Find $(E_h, T_h) \in (V_J \times [0, t_{\max}])^2$ such that

$$\int_\Omega \frac{\partial E_h}{\partial t} u dx + \int_\Omega D_r(E_h, T_h) \nabla E_h \cdot \nabla u dx + \int_{\Gamma_0} \frac{1}{2} E_h u d\sigma \\ - \int_\Omega \sigma_a(T_h)((T_h)^4 - E_h) u dx - \int_{\Gamma_0} 2gu d\sigma = 0, \tag{2.2.6}$$

$$\int_\Omega \frac{\partial T_h}{\partial t} v dx + \int_\Omega D_t(E_h, T_h) \nabla T_h \cdot \nabla v dx + \int_\Omega \sigma_a(T_h)((T_h)^4 - E_h) v dx = 0, \tag{2.2.7}$$

for all $(u, v) \in V_J^2$ and for all $t \in [0, t_{\max}]$.

In above equations, to perform the integration in space, we use a three-point quadrature rule on each triangle in $\mathcal{T}_j$. Because the points where the degrees of freedom are defined and the quadrature points of triangle are the same, we can easily compute the integration on each triangle and

$$\int_K D(x) \phi_i \phi_k dx = \frac{D(x_i)|K|}{3} \delta_{ik} \tag{2.2.8}$$

for all basis functions ϕ_i of V and $K \in \mathcal{T}_j$. Also, because ∇u is a piecewise constant on each triangle in $\mathcal{T}_j$ for all $b \in V$, we compute $|\nabla u|$ needed in D_r exactly.

3. Time integration and nonlinear iteration. In this section, we consider a discretization in time and three nonlinear iterations, i.e., Newton, Picard and inexact Newton iteration.

The time derivatives are discretized as first-order backward differences, with lumping of the mass matrix, leading to an implicit scheme which requires the solution of a nonlinear problem at each time step. This approach is first-order accurate in time, and is chosen merely for convenience, since the principal objective is the study of the solution of the nonlinear system. Higher order temporal discretizations are demonstrated to be worth while in [18].

To solve the nonlinear problem (2.2.6) and (2.2.7) we consider the Picard linearization method and the Newton linearization method. In both methods, we need to solve linear systems to get corrections at each nonlinear iteration step.

The fully implicit Picard linearization method separates the operators into linear parts and nonlinear parts and all nonlinear parts are evaluated at the previous nonlinear iteration level, $k-1$. This results in the following system of equations:

$$\begin{aligned}\int_\Omega \frac{E_h^{n,k}-E_h^{n-1}}{\Delta t}u dx + \int_\Omega D_r^{n,k-1}\nabla E_h^{n,k}\cdot\nabla u dx + \int_{\Gamma_0}\frac{1}{2}E_h^{n,k}u d\sigma \\ - \int_\Omega \sigma_a^{n,k-1}((T_h^{n,k-1})^3 T_h^{n,k} - E_h^{n,k})u dx - \int_{\Gamma_0} 2gu d\sigma = 0,\end{aligned} \tag{3.3.1}$$

$$\begin{aligned}\int_\Omega \frac{T_h^{n,k}-T_h^{n-1}}{\Delta t}v dx + \int_\Omega D_t^{n,k-1}\nabla T_h^{n,k}\cdot\nabla v dx \\ + \int_\Omega \sigma_a^{n,k-1}((T_h^{n,k-1})^3 T_h^{n,k} - E_h^{n,k})v dx = 0,\end{aligned} \tag{3.3.2}$$

for all $(u,v)\in V_J^2$. Because (3.3.1) and (3.3.2) are linear systems in $(E_h^{n,k}, T_h^{n,k})$, we can easily calculate their Jacobian.

To get the corrections $(\delta E, \delta T)$ in the Picard Method at level k, we solve the following linear systems.

$$\begin{aligned}\int_\Omega \frac{\delta E}{\Delta t}u dx + \int_\Omega D_r^{n,k-1}\nabla \delta E\cdot\nabla u dx + \int_{\Gamma_0}\frac{1}{2}\delta E u d\sigma \\ - \int_\Omega \sigma_a^{n,k-1}((T_h^{n,k-1})^3\delta T - \delta E)u dx = F_E^{n,k-1}(u),\end{aligned} \tag{3.3.3}$$

$$\begin{aligned}\int_\Omega \frac{\delta T}{\Delta t}v dx + \int_\Omega D_t^{n,k-1}\nabla \delta T\cdot\nabla v dx \\ + \int_\Omega \sigma_a^{n,k-1}((T_h^{n,k-1})^3\delta T - \delta E)v dx = F_T^{n,k-1}(v),\end{aligned} \tag{3.3.4}$$

for all $(u,v)\in V_J^2$ where

$$\begin{aligned}F_E^{n,k}(u) = -\int_\Omega \frac{E_h^{n,k}-E_h^{n-1}}{\Delta t}u dx - \int_\Omega D_r^{n,k}\nabla E_h^{n,k}\cdot\nabla u dx \\ - \int_{\Gamma_0}\frac{1}{2}E_h^{n,k}u d\sigma + \int_\Omega \sigma_a^{n,k}((T_h^{n,k})^4 - E_h^{n,k})u dx + \int_{\Gamma_0} 2gu d\sigma,\end{aligned} \tag{3.3.5}$$

$$\begin{aligned}F_T^{n,k}(v) = -\int_\Omega \frac{T_h^{n,k}-T_h^{n-1}}{\Delta t}v dx - \int_\Omega D_t^{n,k}\nabla T_h^{n,k}\cdot\nabla v dx \\ - \int_\Omega \sigma_a^{n,k}((T_h^{n,k})^4 - E_h^{n,k})v dx.\end{aligned} \tag{3.3.6}$$

For the fully implicit Newton linearization method it is somewhat more complicated to compute the Jacobian at approximate solution points. To get the Jacobian, we have to calculate the derivatives of the system with respect to (ϕ_i, ψ_i) for all basis functions in $V_J \times V_J$.

As the result of differentiation with respect to (ϕ_i, ψ_i), to get the corrections $(\delta E, \delta T)$ in Newton's Method at level k, we solve the following linear systems.

$$\begin{aligned}
&\int_\Omega \frac{\delta E}{\Delta t} u dx + \int_\Omega D_r^{n,k-1} \nabla \delta E \cdot \nabla u dx + \int_\Omega D_{r,E}^{n,k-1} \delta E \nabla E_h^{n,k-1} \cdot \nabla u dx \\
&\quad + \int_\Omega D_{r,T}^{n,k-1} \delta T \nabla E_h^{n,k-1} \cdot \nabla u dx + \int_{\Gamma_0} \frac{1}{2} \delta E u d\sigma \\
&\quad - \int_\Omega \sigma_a^{n,k-1} \left(1 + 3\frac{E_h^{n,k-1}}{T_h^{n,k-1}}\right) \delta T u dx + \int_\Omega \sigma_a^{n,k-1} \delta E u dx = F_E^{n,k-1}(u),
\end{aligned} \tag{3.3.7}$$

$$\begin{aligned}
&\int_\Omega \frac{\delta T}{\Delta t} v dx + \int_\Omega D_t^{n,k-1} \nabla \delta T \cdot \nabla v dx + \int_\Omega D_{t,T}^{n,k-1} \delta T \nabla T_h^{n,k-1} \cdot \nabla v dx \\
&\quad + \int_\Omega \sigma_a^{n,k-1} \left(1 + 3\frac{E_h^{n,k-1}}{T_h^{n,k-1}}\right) \delta T v dx - \int_\Omega \sigma_a^{n,k-1} \delta E v dx = F_T^{n,k-1}(v),
\end{aligned} \tag{3.3.8}$$

for all $(u, v) \in V^2$ where

$$\begin{aligned}
D_{r,E}^{n,k} &= \frac{(D_r^{n,k})^2 |\nabla E_h^{n,k}|}{(E_h^{n,k})^2} + \frac{(D_r^{n,k})^2}{E_h^{n,k}} \frac{\partial |\nabla E_h^{n,k}|}{\partial (E_h^{n,k})_i}, \\
D_{r,T}^{n,k} &= \frac{9(D_r^{n,k})^2}{(T_h^{n,k})^4}, \\
D_{t,T}^{n,k} &= \kappa \frac{5}{6} (T_h^{n,k})^{3/2},
\end{aligned}$$

where $\frac{\partial |\nabla E_h^{n,k}|}{\partial (E_h^{n,k})_i}$ can be easily evaluated on each triangle in $\mathcal{T}_J$.

After linearization, we have to solve the linear systems

$$\mathbf{J}^{k-1} \begin{pmatrix} \delta E \\ \delta T \end{pmatrix} = \begin{pmatrix} F_E^{n,k-1} \\ F_T^{n,k-1} \end{pmatrix} \tag{3.3.9}$$

for each step where $\mathbf{J}^{k-1}$ is a Jacobian, which is computed by Picard's method or Newton's method.

In either method, we need for robustness to control the step length α where

$$\begin{pmatrix} E_h^{n,k} \\ T_h^{n,k} \end{pmatrix} = \begin{pmatrix} E_h^{n,k-1} \\ T_h^{n,k-1} \end{pmatrix} + \alpha \begin{pmatrix} \delta E \\ \delta T \end{pmatrix}.$$

In this study, we control the step length by simply halving α until the residual of the updated solution is less than the previous residual. In this control, we sometimes fail to get a proper step length, so we stop at a fixed step length and perform the next nonlinear iteration. If the number of failures exceeds a fixed number, then we go to next time steps by using the best approximation, which has the smallest nonlinear residual.

REMARK 3.1. *The Newton method has, asymptotically, a second order convergence for nonlinear problems and the Picard method has only a first order convergence. However the resulting linear problem of the Picard method is more easily solved than that of the Newton method because the Picard method lacks the convection term as described in ref. [7].*

To improve the efficiency of the Newton method, we can use an inexact Newton method [8]. When the Newton iteration is "far" from convergence (i.e., the residual is large) there is no reason to solve the linear system accurately. However, when the Newton iteration is "close" (i.e., the residual is "small") the convergence rate of Newton's method is tightly coupled to the accuracy of the linear solution. To adjust the amount of work done in the linear solve (via a convergence tolerance) we employ an inexact Newton method.

In the inexact Newton approach, the convergence criteria for the linear solver is proportional to the residual in the nonlinear iteration. In equation form this is

$$\left\| \mathbf{J}^{k-1} \begin{pmatrix} \delta E \\ \delta T \end{pmatrix} - \begin{pmatrix} F_E^{n,k-1} \\ F_T^{n,k-1} \end{pmatrix} \right\| \leq \gamma_2 \left\| \begin{pmatrix} F_E^{n,k-1} \\ F_T^{n,k-1} \end{pmatrix} \right\|, \tag{3.3.10}$$

where $\gamma_2 = 1.0 \times 10^{-2}$ is the value used in this study unless otherwise noted. We note that [13] shows how to adaptively select γ_2 to recover asymptotically full second order convergence.

4. PGMRES and multigrid preconditioning. In this section, we explain PGMRES, which is a combination of a Krylov-based linear iterative method, and multigrid, which is well known as a successful preconditioner, as well as a scalable solver even in unaccelerated form, for many problems.

GMRES [23] is a well known solver for non-Hermitian problems. In practice, GMRES can be restarted after m steps, where m is some fixed integer parameter, to save storage by accepting a generally less rapid convergence.

We describe the restarted PGMRES for solving

$$A_J x = b \tag{4.4.1}$$

with preconditioning matrix B_J.

PGMRES(m) Algorithm 4.1.

(1) Start : Choose x_0 and compute $r_0 = B_J(b - A_J x_0)$, $\beta = \|r_0\|_2$ and $v_1 = r_0/\beta$.

(2) Iterate : For $j = 1, \ldots, m$ do:

Compute $w := B_J A_J v_j$

For $i = 1, \ldots, j$, do:

$$h_{i,j} := (w, v_i)$$
$$w := w - j_{i,j} v_i$$

Enddo

Compute $h_{j+1,j} = \|w\|_2$ and $v_{j+1} = w/h_{j+1,j}$

Enddo

(3) Form the approximation solution:

Define $V_m := [v_1, \ldots, v_m]$,

$$\bar{H}_m = \{h_{i,j}\}_{1 \leq i \leq j+1; 1 \leq j \leq m}$$

and set $x_m = x_0 + V_m y_m$, where y_m minimizes $\|\beta e_1 - \bar{H}_m y\|$, $y \in R^m$.

(4) Restart:

Compute $r_m = B_J(b - A_J x_m)$; if satisfied then stop

else compute $x_0 := x_m$, $\beta = \|r_m\|$ and $v_1 = r_m/\beta$ and go to (2).

Arnoldi iteration constructs an orthogonal basis of the left preconditioned Krylov subspace

$$\text{Span}\{r_0, B_J A_J r_0, \ldots, (B_J A_J)^{m-1} r_0\}.$$

It uses a modified Gram-Schmidt process, in which the new vector to be orthogonalized is obtained from the previous vector in the process. All residual vectors and their norms that are computed by the algorithm

correspond to the preconditioned residuals, namely, $z_m = B_J(b - A_J x_m)$, instead of the original (unpreconditioned) residual $b - A_J x_m$. In addition, there is no easy access to these unpreconditioned residuals, unless they are computed explicitly. So we monitor these preconditioned residuals to stop PGMRES iteration to solve linear problem.

Next, we consider Multigrid Preconditioner B_J.

To define a multigrid method, we need to define intergrid transfer operators between nonconforming finite element spaces. Due to the non-nestedness of nonconforming spaces, there is not a natural intergrid transfer operator. In previous studies of nonconforming multigrid method[1, 5, 6, 9], average value of two adjacent elements are used to set the value of a node. A nonconforming multigrid method with this intergrid transfer operator is a good solver for linear systems and some nonlinear systems that have smooth nonlinear coefficients.

To get the coarse level approximate linear system for (3.3.9), we need coarse level approximations of $(E_h^{n,k-1}, T_h^{n,k-1})$ and (E_h^{n-1}, T_h^{n-1}). If the approximate solution $(E_h^{n,k-1}, T_h^{n,k-1})$ varies rapidly in space, then some coarse level approximations of $(E_h^{n,k-1}, T_h^{n,k-1})$ may have negative values. However $(E_h^{n,k-1}, T_h^{n,k-1})$ are required to be positive for the computation of $D_t^{n,k-1}$. Either we cannot generate the coarse level systems or they may become nearly singular, making it hard to solve the coarse level problems.

To overcome these difficulties, we use a new and simple intergrid transfer operator called the covolume-based intergrid transfer operator, which preserves only piecewise constant functions [15]. It is well known that, to get a good convergence factor in multigrid algorithms, intergrid transfer operators should preserve higher order functions [19]. Therefore the multigrid method with this intergrid transfer operator converges slowly compared to average value intergrid operator to solve linear systems. However preservation of positivity of nodal values of the fields is critical. So, we use the covolume-based intergrid transfer operator to obatain the coarse level systems and the average value intergrid operator to interpolate the solution between levels (coarse-to-fine and fine-to-coarse) when solving the linear systems in Picard'method or Newton's method.

Let $A_j; (V_j)^2 \to (V_j)^2$, $j = 1, \ldots, J$ be the discretization operator on level j and $I_j : (V_{j-1})^2 \to (V_j)^2$, $j = 2, \ldots, J$, be the coarse-to-fine intergrid transfer operator. Also, we define the fine-to-coarse intergrid transfer operator $P_{j-1}^0 : (V_j)^2 \to (V_{j-1})^2$ by

$$(I_j v, w) = (v, P_{j-1}^0 w), \quad \forall v \in (V_{j-1})^2, \forall w \in (V_j)^2.$$

Finally, let $R_j : (V_j)^2 \to (V_j)^2$ for $j = 1, \ldots, J$ be the linear smoothing operators, let R_j^T denote the adjoint of R_j with respect to the $(\cdot, \cdot)$ inner product, and define

$$R_j^{(l)} = \begin{cases} R_j, & l \text{ odd}, \\ R_j^T, & l \text{ even}. \end{cases}$$

Following [2], the multigrid operator $B_j : (V_j)^2 \to (V_j)^2$ is defined recursively as follows.

Multigrid Algorithm 4.2. Let $1 \le j \le J$ and p be a positive integer. Set $B_1 = A_1^{-1}$. Assume that B_{j-1} has been defined and define $B_j g$ for $g \in (V_j)^2$ by

(1) Set $x^0 = 0$ and $q^0 = 0$.

(2) Define x^l for $l = 1, \ldots, m(j)$ by

$$x^l = x^{l-1} + R_k^{(l+m(j))}(g - A_j x^{l-1}).$$

(3) Define $y^{m(j)} = x^{m(j)} + I_j q^p$, where q^i for $i = 1, \ldots, p$ is defined by

$$q^i = q^{i-1} + B_{j-1}[P_{j-1}^0(g - A_j x^{m(j)}) - A_{j-1} q^{i-1}].$$

(4) Define y^l for $l = m(j) + 1, \ldots, 2m(j)$ by

$$y^l = y^{l-1} + R_j^{(l+m(j))}(g - A_j y^{l-1}).$$

(5) Set $B_j g = y^{2m(j)}$.

In Multigrid algorithm 4.2, $m(j)$ gives the number of pre- and post-smoothing iterations and can vary as a function of j. If $p = 1$, we have a V-cycle multigrid algorithm. If $p = 2$, we have a W-cycle multigrid algorithm. Other versions of multigrid algorithms without pre- or post-smoothing iterative can be analyzed similarly. A variable V-cycle multigrid algorithm is that for which the number of smoothing $m(j)$ increases exponentially as j decreases (i.e., $p = 1$ and $m(j) = 2^{J-j}$).

REMARK 4.1. *One can use the multigrid algorithm to solve the systems as a free-standing iterative method. Usually, one uses V-cycle and W-cycle multigrid algorithms to this end and uses V-cycle and variable V-cycle multigrid method as preconditioners of Krylov-type methods such as PCG, because, when A_j is symmetric positive definite, the V-cycle multigrid operator B_j is a symmetric positive definite operator on $(V_j)^2$, but the W-cycle multigrid operator is not in generally [3]. Many researchers show that convergence of W-cycle multigrid for the nonconforming and conforming cases and V-cycle multigrid for the conforming case are good preconditioners [1, 2, 5, 6, 9, 14, 16, 25]. In this problem, we use V-cycle multigrid method as a preconditioner of GMRES.*

5. Algorithm performance and results. In this section, we study the performance of the Newton, Picard, and inexact Newton methods on P_1 nonconforming finite element method on two model problems with the only difference between the problems being homogeneity. In the two examples, we use the same triangulations, namely 12800 triangles, 19296 edges, and 6497 vertices. Because nodes are on midpoints of edges in a P_1 nonconforming method, the number of degrees of freedom of this problem is 38592.

For problem 1, we consider a homogeneous material with atomic number $z = 1$ and $\kappa = 0.01$ on the whole domain. The initial conditions are $E^0 = 1.0 \times 10^{-5}$ and $T^0 = (E^0)^{0.25}$. The problem is run out to time $t = 3.0$ and nonlinear convergence tolerance within a time step is defined as $\|\mathbf{F}(\mathbf{u}^k)\|_2 \leq 1.0 \times 10^{-6}$ for problem 1. We run with several time steps of 0.001, 0.002, 0.005, and 0.01.

In Figure 3, we plot the contours of temperature T at $t = 1.0, 2.0, 3.0$. Table 1 compares linear solve requirements and nonlinear iterations. Figure 4 depicts the nonlinear convergence behavior of Newton method, Picard method, and Inexact Newton method at time $t = 1.0$.

Figure 3 shows that contours of temperature propagate parallel to the inlet boundary and reproduce on an unstructured grid the propagation of the one-dimensional case. Table 1 and Figure 4 show that Newton's Method is very efficient compared to Picard's method, and slightly more efficient compared to the inexact Newton method, in terms of nonlinear iterations per time step.

Inexact Newton needs more nonlinear iterations in comparison to Newton's method, but has the best performance overall because this method needs the smallest number of linear iterations. Also, Table 1 shows that the number of linear iterations in each nonlinear iteration of the Picard method is smaller than that of the Newton Method. This means that the linear systems from Picard's method are more easily solved than the linear systems from Newton method.

In Table 2, we report the accuracy as a function of time steps by the L^2-error of the solution which is defined as $\|u - u_{\text{base}}\|_2$ where u_{base} is obtained by using a time step 0.0001. This result shows that the L^2-error in time is first order.

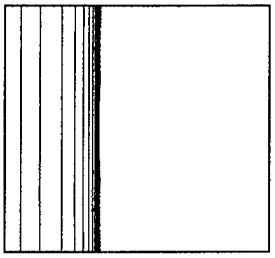

(a) $t = 1.0$

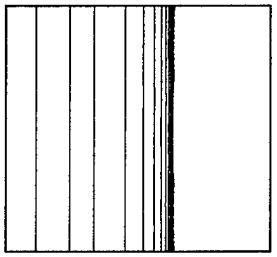

(b) $t = 2.0$

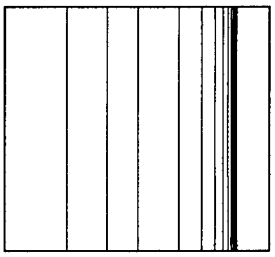

(c) $t = 3.0$

FIG. 3. *Contour of Temperature of Problem 1*

For problem 2, we consider an inhomogeneous material with atomic number $z = 10$ inside the box and $z = 1.0$ outside, as shown in Figure 5. We changed the nonlinear convergence tolerance within a time step to be $\|\mathbf{F}(\mathbf{u}^k)\|_2 \leq 1.0 \times 10^{-4}$ to reduce the simulation times.

In Figure 6, we plot the contour of temperature T at $t = 1.0, 2.0, 3.0, 4.0, 5.0$. Table 3 compares linear solve requirements, nonlinear iterations, and number of failures to meet the convergence tolerance. Figures 8, 9, 10 demonstrate the nonlinear convergence behavior of the Newton, Picard, and inexact Newton methods at times $t = 1.0$, $t = 2.5$, and $t = 4.0$.

As energy propagates, temperatures rapidly change near the front and near the layer where the two different materials meet. As more time passes, the temperature smoothly propagates. Figures 8, 9, 10 show that there are many step length controls to get the solution of the nonlinear problem when the solution changes rapidly ($t = 1.0, t = 2.5$) but there is no need for step length control when the solution is smooth ($t = 4.0$) in any of the three methods.

TABLE 1. *Algorithm performance as a function of time step for problem 1 and time period of 3.0*

Method	dt	# of dt	tot # nonlinear	ave # nonlin iter /dt	tot # linear	ave # lin /dt	ave # lin /nonlin
Newton method	0.001	3000	6226	2.1	49851	16.6	8.0
	0.002	1500	4116	2.7	38970	26.0	9.5
	0.005	600	2120	3.5	28197	46.8	13.3
	0.01	300	1334	4.4	21986	73.7	16.5
Picard Method	0.001	3000	24935	8.3	181227	60.4	7.3
	0.002	1500	15389	10.3	126152	84.1	8.2
	0.005	600	7784	13.0	70165	116.9	9.0
	0.01	300	5320	17.7	46194	154.0	8.7
Inexact Newton Method	0.001	3000	8648	2.9	28468	9.5	3.3
	0.002	1500	4534	3.0	15928	10.6	3.5
	0.005	600	2254	3.8	9878	16.6	4.4
	0.01	300	1450	4.8	7761	25.9	5.4

TABLE 2. *L^2-error at $t = 3.0$*

time steps	L^2(error)
0.001	0.00884
0.002	0.01796
0.005	0.04060
0.01	0.06676

Figure 6 shows that the solution of the nonconforming finite element method is very similar to the solution of finite volume method with edge-based flux limiter [20].

In the aspect of performance, the behavior of problem 2 is similar to problem 1 with the exception that problem 1 does not require step length control.

To estimate the accuracy as a function of time step size, we report the L^2-error of the solution in Table 4 (based on an accurate solution with $dt = 0.0001$). The relative L^2-error of simulations with $dt = 0.002$, 0.005, 0.01 compared to the L^2-error of $dt = 0.001$ is ploted as a function of time in Figure 7. These results show that the L^2-error in time is first order at the beginning of simulation until $t = 3.0$ but gradually deteriorates. This deterioration may be introduced by the nonlinear convergence error within a time step because the accumulation of the nonlinear convergence error will dominate other errors (space and time discretization error) as time steps grows. If we use a finer nonlinear convergence tolerance, then we can delay this deterioration to longer time.

6. Conclusions. We solved unsteady implicit nonlinear radiation diffusion problems by an unstructured P_1 nonconforming finite element method. P_1 nonconforming finite element methods resolve very sharp changes of energies on the heterogeneous domains, similarly to results of the finite volume method with an edge-based flux limiter. The inexact Newton method has the best performance overall and Preconditioned GMRES with nonconforming multigrid preconditioner to solve linear problems works well. In P_1 nonconforming multigrid, the covolume-based intergrid transfer operators are useful to solve radiation transport

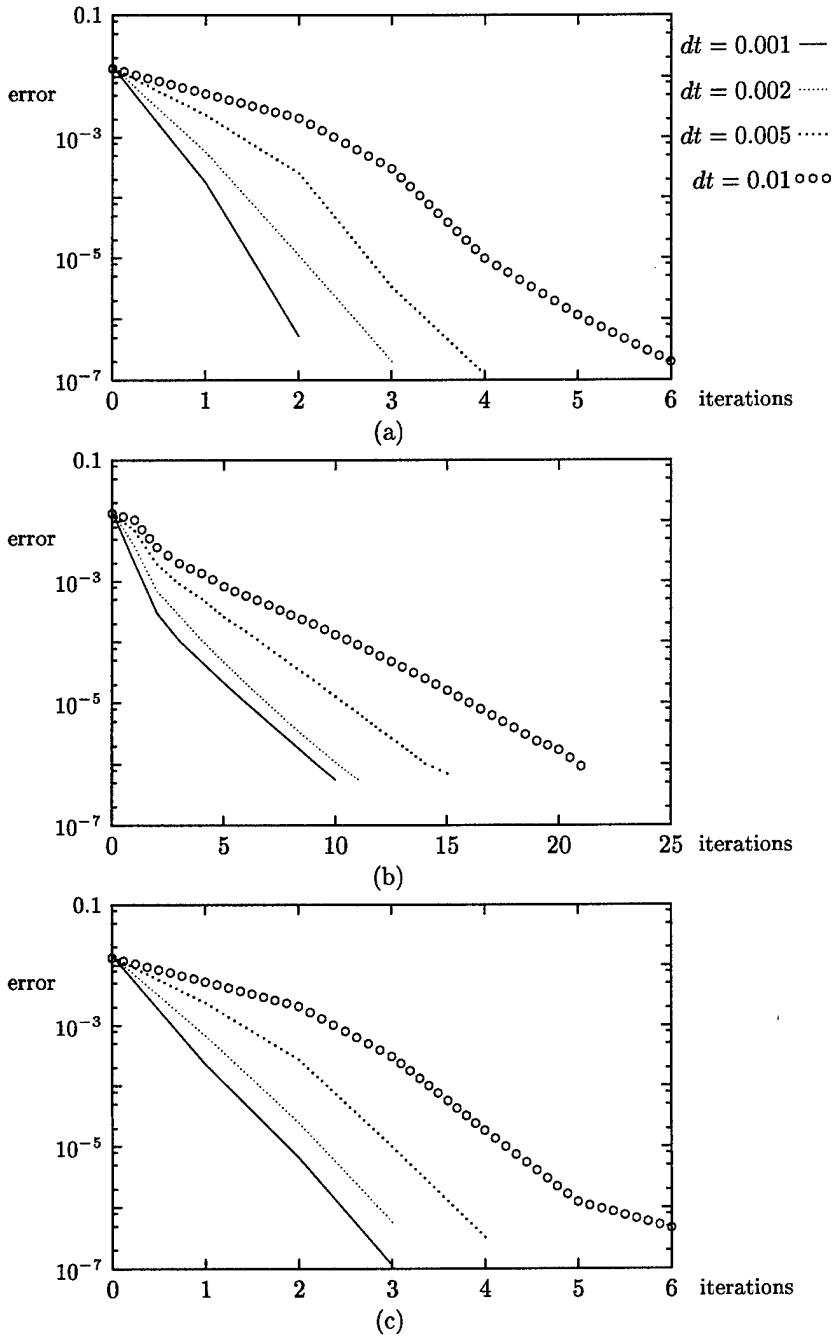

FIG. 4. *Convergence plot on problem 1 at time* $t = 1.0$, *(a) Newton Method, (b) Picard Method, (c) Inexact Newton Method*

problems because the positivity preserving property is needed.

Acknowledgments. The author would like to thank D. E. Keyes of Old Dominion University for his valuable advice in the preparation of this paper.

REFERENCES

[1] D. BRAESS AND R. VERFÜRTH, *Multigrid methods for nonconforming finite element methods*, SIAM J. Numer. Anal., **27**(1990), pp. 979–986.

[2] J. BRAMBLE, Multigrid Methods, Pitman, London, 1993.

[3] J. BRAMBLE, J. PASCIAK, AND J. XU, *The analysis of multigrid algorithms with non-nested spaces or non-inherited quadratic forms*, Math. Comp., **56**(1991), pp. 1–34.

[4] A. BRANDT, *Multigrid techniques with applications to fluid dynamics: 1984 guide*, in VKI Lecture Series, Mar. 1984, 176 pp.

[5] S. BRENNER, *An optimal-order multigrid method for P_1 nonconforming finite elements*, Math. Comp. **52**(1989), pp. 1–15.

[6] S. BRENNER, *Convergence of nonconforming multigrid methods without full elliptic regularity*, Math. Comp., **68**(1999), pp. 25–53.

[7] P. N. BROWN AND C. S. WOODWARD, *Preconditioning Strategies for Fully Implicit Radiation Diffusion with Material-Energy Transfer*, SIAM Journal on Scientific Computing, **23**(2001), pp. 499–516.

[8] X. C. CAI AND D. E. KEYES, *Nonlinearly Preconditioned Inexact Newton Algorithms*, SIAM J. Sci. Comput. **24**(2002), pp. 183–200.

[9] Z. CHEN, *The analysis of intergrid transfer operators and Multigrid methods for nonconforming finite elements*, ETNA **5**(1998), pp. 78–96.

[10] S. H. CHOU, *Analysis and convergence of a covolume method for the generalized Stokes Problem*, Math. Comp. **66**(1989), pp. 85–104.

[11] M. CROUZEIX AND P. -A. RAVIART, *Conforming and nonconforming finite element method for solving the stationary Stokes equations. I*, RAIRO R-3 (1973), pp 33-75.

[12] M. D'AMICO, *A Newton-Raphson approach for nonlinear diffusion equations in radiation hydrodynamics*, J. Quant. Spec. and Rad. Trans., **54**(1995), pp. 655-669.

[13] S. C. EISENSTAT AND H. F. WALKER, *Globally convergence inexact Newton methods*, SIAM J. Optimization **4**(1994), pp. 393–422.

[14] W. HACKBUSH, *Multigrid Methods and Applications*, Springer-Verlag, Berlin, Germany, 1985.

[15] K. S. KANG, *Covolume-based intergrid transfer operator in P_1 nonconforming multigrid method*, ICASE Report No. 2002-15, NASA/CR-2002-211655, 2002.

[16] K. S. KANG AND S. Y. LEE, *New intergrid transfer operator in multigrid method for P_1-nonconforming finite element method*, Applied Mathematics and Computation, **100**(1999), pp. 139–149.

[17] D. A. KNOLL, W. J. RIDER, AND G. L. OLSON, *An efficient nonlinear solution method for nonequilibrium radiation diffusion*, J. Quant. Spec. and Rad. Trans., **63**(1999), pp. 15–29.

[18] D. A. KNOLL, W. J. RIDER, AND G. L. OLSON, *Nonlinear convergence, accuracy, and time step control in nonequilibrium radiation diffusion*, J. Quant. Spec. and Rad. Trans., **70**(2001), pp. 25–36.

[19] D. J. MAVRIPLIS, *Multigrid techniques for unstructured meshes*, in VKI Lecture Series VKI-LS 1995-02, Mar. 1995.

[20] D. J. MAVRIPLIS, *An Assessment of Linear Versus Non-linear Multigrid Methods for Unstructured Mesh Solvers*, ICASE Report No. 2001-12, Journal of Computational Physics, **175**(2002), pp. 302-325.

[21] V. A. MOUSSEAU, D. A. KNOLL, and W. J. Rider, *Physics-based preconditioning and the Newton-Krylov method for non-equilibrium radiation diffusion*, Journal of Computational Physics,

160(2000), pp. 743–765.

[22] W. J. RIDER, D. A. KNOLL, AND G. L. OLSON, *A Multigrid Newton-Krylov Method for Multimaterial Equilibrium Radiation Diffusion*, Journal of Computational Physics, **152**(1999), pp. 164–191.

[23] Y. SAAD AND M. H. SCHULTZ, *GMRES: A Generalized Minimal Residual Algorithm for solving nonsymmetric linear systems*, SIAM J. Sci. Stat. Comput., **7**(1986), pp. 856–869.

[24] B. SU AND G. L. OLSON, *Benchmark results for the non-equilibrium Marshak diffusion problem*, J. Quant. Spec. and Rad. Trans. **56**(1996), pp. 337–351.

[25] P. WESSELING, *An Introduction to Multigrid Methgods*, Wiley, Chichester, U.K., 1992.

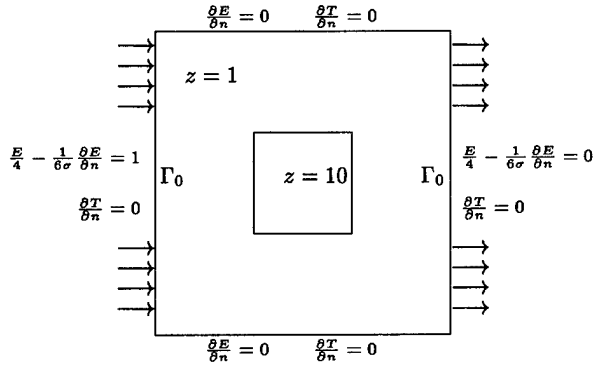

FIG. 5. *Domain of inhomogeneous material*

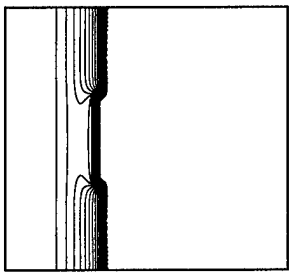

(a) $t = 1.0$

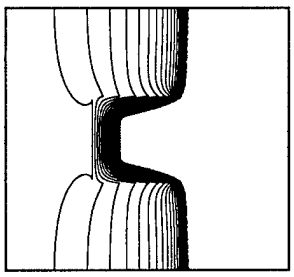

(b) $t = 2.0$

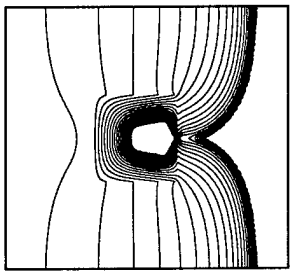

(c) $t = 3.0$

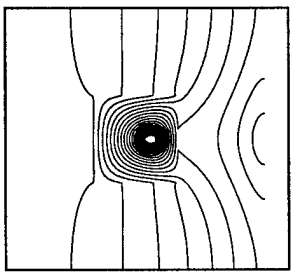

(d) $t = 4.0$

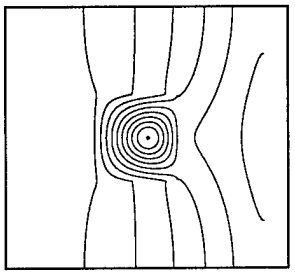

(e) $t = 5.0$

FIG. 6. *Contour of Temperature of Problem 2*

TABLE 3. *Algorithm performance as a function of time step for problem 2 and time period of 5.0*

Method	dt	# of dt	tot # nonlinear	ave # nonlin iter /dt	tot # linear	ave # lin /dt	ave # lin /nonlin
	0.001	5000	11980	2.4	118186	23.6	9.9
Newton	0.002	2500	6745	2.7	83839	33.5	12.4
method	0.005	1000	4314	4.3	76436	76.4	17.7
	0.01	500	2975	6.0	68770	137.5	23.1
	0.001	5000	34074	6.8	274482	54.9	8.1
Picard	0.002	2500	21391	8.6	204722	81.9	9.6
Method	0.005	1000	12083	12.1	145875	145.9	12.1
	0.01	500	7891	15.8	105234	210.5	13.3
Inexact	0.001	5000	11701	2.3	42669	8.5	3.6
Newton	0.002	2500	7045	2.8	32703	13.1	4.6
Method	0.005	1000	4559	4.6	30183	30.2	6.6
	0.01	500	3259	6.5	27516	55.0	8.4

TABLE 4. *L^2-error at $t = 5.0$*

time steps	L^2(error)
0.001	0.00017
0.002	0.00019
0.005	0.00048
0.01	0.00108

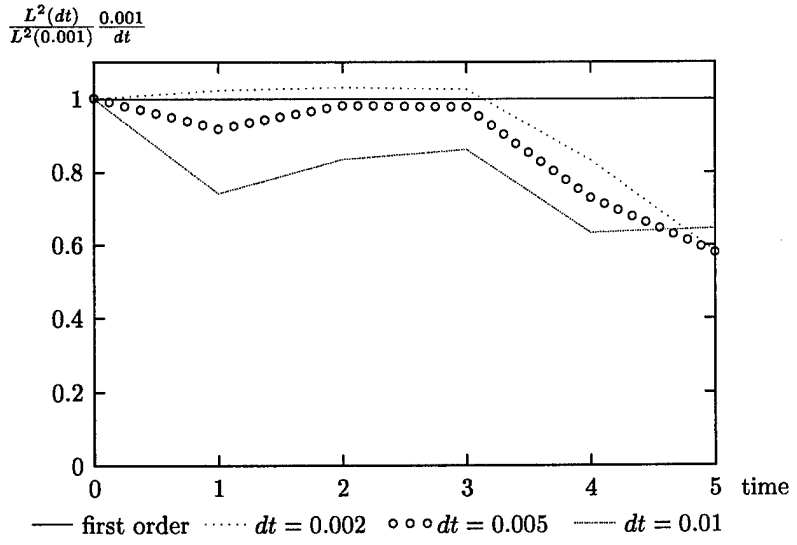

FIG. 7. *The relative L^2-error compared with L^2-error of $dt = 0.001$ $(L^2(dt)/L^2(dt = 0.001) \times 0.001/dt)$*

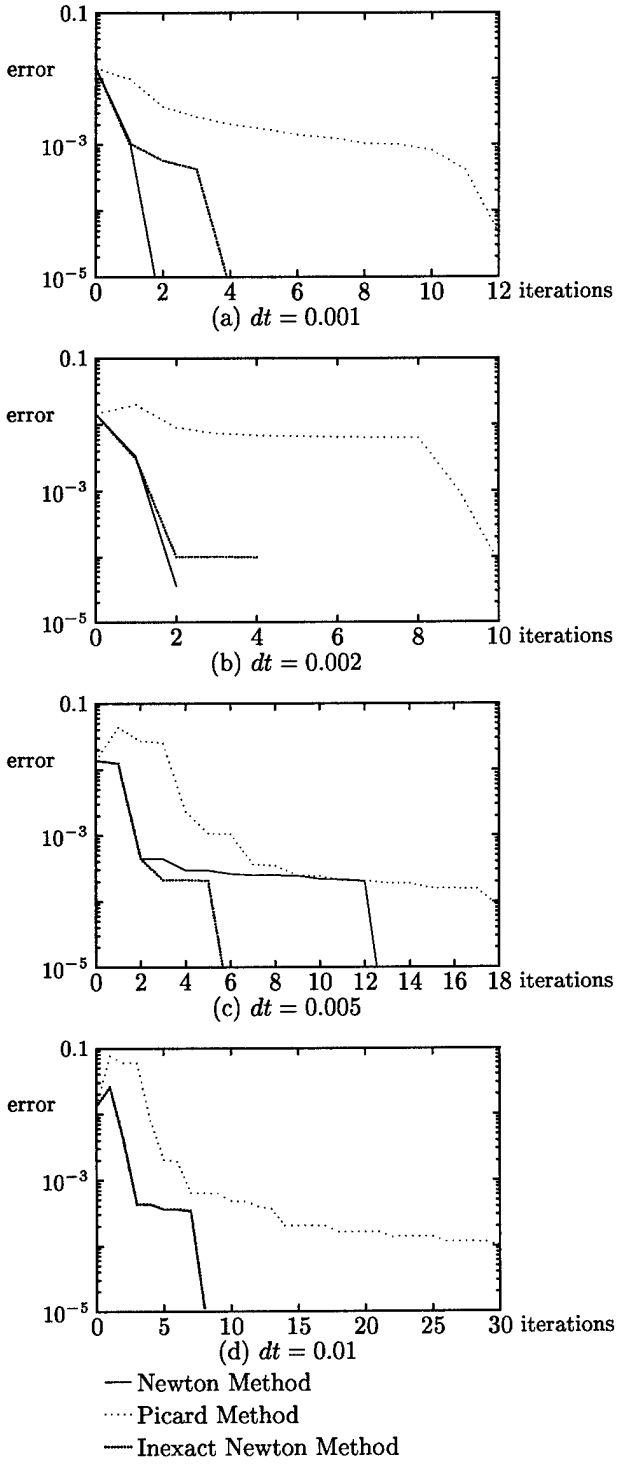

FIG. 8. *Convergence plot at time* $t = 1.0$

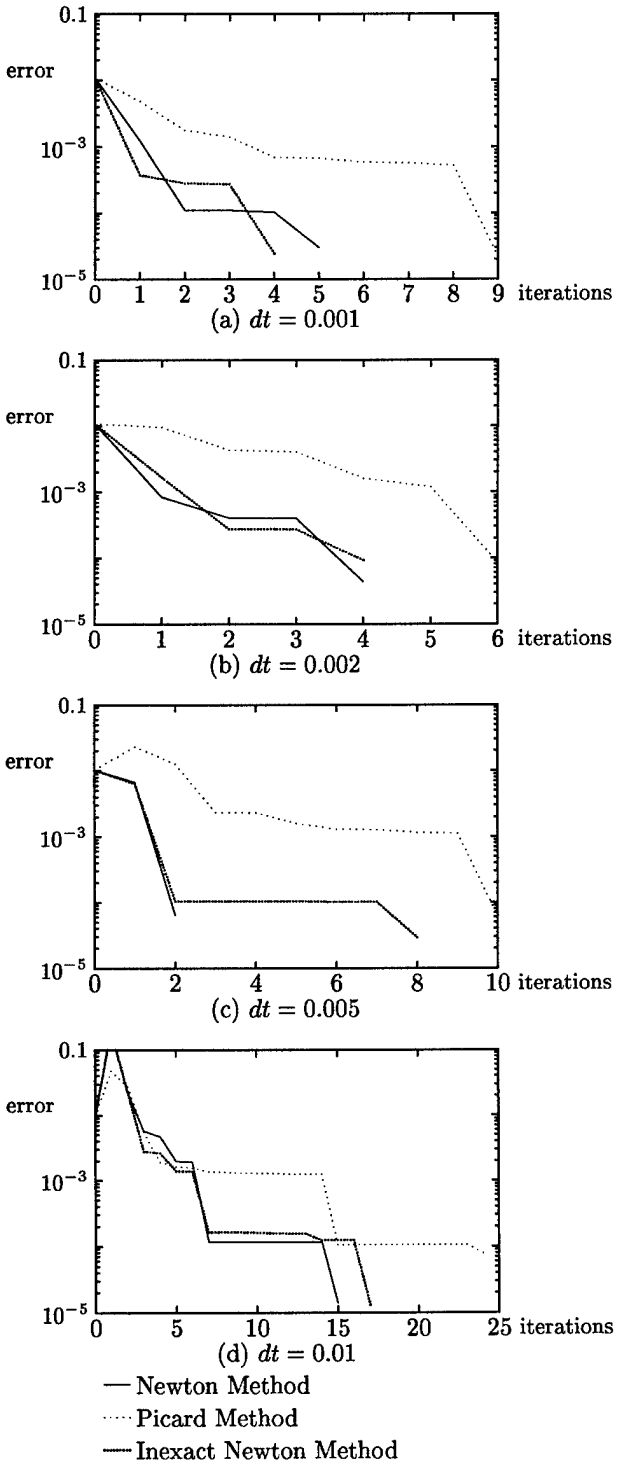

FIG. 9. *Convergence plot at time* $t = 2.5$

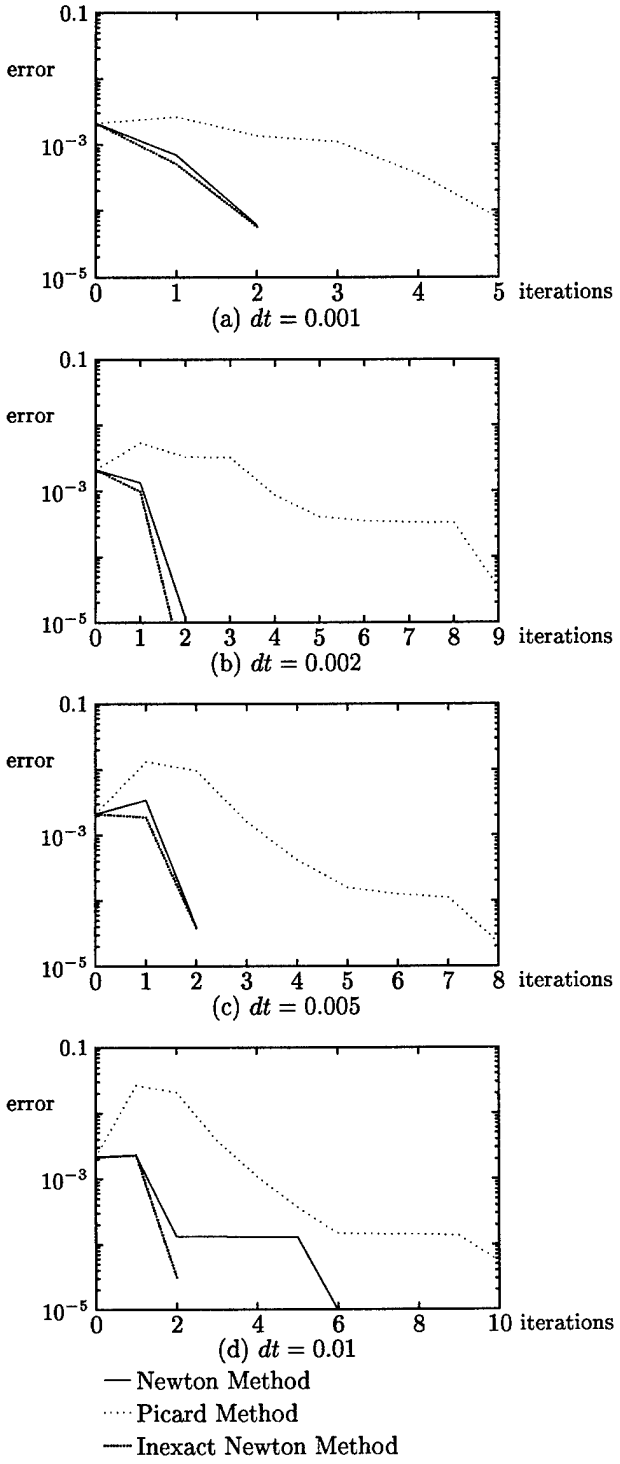

FIG. 10. *Convergence plot at time* $t = 4.0$

REPORT DOCUMENTATION PAGE

Form Approved
OMB No. 0704-0188

1. AGENCY USE ONLY *(Leave blank)*	2. REPORT DATE	3. REPORT TYPE AND DATES COVERED
	August 2002	Contractor Report

4. TITLE AND SUBTITLE
P_1 NONCONFORMING FINITE ELEMENT METHOD FOR THE SOLUTION OF RADIATION TRANSPORT PROBLEMS

5. FUNDING NUMBERS
C NAS1-97046
WU 505-90-52-01

6. AUTHOR(S)
Kab Seok Kang

7. PERFORMING ORGANIZATION NAME(S) AND ADDRESS(ES)
ICASE
Mail Stop 132C
NASA Langley Research Center
Hampton, VA 23681-2199

8. PERFORMING ORGANIZATION REPORT NUMBER
ICASE Report No. 2002-28

9. SPONSORING/MONITORING AGENCY NAME(S) AND ADDRESS(ES)
National Aeronautics and Space Administration
Langley Research Center
Hampton, VA 23681-2199

10. SPONSORING/MONITORING AGENCY REPORT NUMBER
NASA/CR-2002-211762
ICASE Report No. 2002-28

11. SUPPLEMENTARY NOTES
Langley Technical Monitor: Dennis M. Bushnell
Final Report
Submitted to a Special Issue of the SIAM Journal of Scientific Computing.

12a. DISTRIBUTION/AVAILABILITY STATEMENT
Unclassified–Unlimited
Subject Category 64
Distribution: Nonstandard
Availability: NASA-CASI (301) 621-0390

12b. DISTRIBUTION CODE

13. ABSTRACT *(Maximum 200 words)*
The simulation of radiation transport in the optically thick flux-limited diffusion regime has been identified as one of the most time-consuming tasks within large simulation codes. Due to multimaterial complex geometry, the radiation transport system must often be solved on unstructured grids. In this paper, we investigate the behavior and the benefits of the unstructured P_1 nonconforming finite element method, which has proven to be flexible and effective on related transport problems, in solving unsteady implicit nonlinear radiation diffusion problems using Newton and Picard linearization methods.

14. SUBJECT TERMS
nonconforming finite elements, radiation transport, inexact Newton linearization, multigrid preconditioning

15. NUMBER OF PAGES
24

16. PRICE CODE
A03

17. SECURITY CLASSIFICATION OF REPORT	18. SECURITY CLASSIFICATION OF THIS PAGE	19. SECURITY CLASSIFICATION OF ABSTRACT	20. LIMITATION OF ABSTRACT
Unclassified	Unclassified		